

# Comparison Between Different Approaches to Interplanetary Mission Design

GIANCARLO GENTA, P. FEDERICA MAFFIONE  
Department of Mechanical and Aerospace Engineering  
Politecnico di Torino  
Corso Duca degli Abruzzi 24, Torino  
ITALY  
giancarlo.genta@polito.it <http://www.giancarlogenta.it>

*Abstract:* - A general purpose design code for interplanetary missions is presented. The code, based on the MatLab environment, allows to deal with both impulsive propulsion (using the patched conics approach) and low continuous thrust. In the latter case, the solver developed specifically for this program is based on an indirect method. More general standard solvers, based on direct methods, like the FALCON.m code can, however, be used. The present paper shows a comparison between different approaches and methods, to evaluate the reliability and accuracy of the proposed code in different applications, by using a number of examples. Finally, some extensions of the code, which are planned for the future, are mentioned.

*Key-Words:* - Interplanetary mission design, Interplanetary trajectories, Launch opportunities, Interplanetary mission optimization

## 1 Introduction

To design an interplanetary mission, it is necessary to make some preliminary choices, some of them related to the duration of the mission and the launch window. Once the starting and arrival dates have been stated, the next step is to find a trajectory that satisfies the requirements of the mission (e.g. minimum-time trajectory, minimum-propellant trajectory, etc.).

The computation of the trajectory can be performed at different accuracy levels: as an initial approximation, the planetary orbits may be assumed to be circular and coplanar and the problem may be modelled as a two-body problem; then, more accurate ephemerides of the solar system can be used and the presence of the various bodies of the solar system can be accounted for. To further improve the accuracy, other effects like the pressure of the solar radiation on the spacecraft can be also considered.

The more simplified is the approach used, the greater is the number of alternatives which may realistically be considered: the study usually starts with very simplified computations to proceed towards more and more accurate solutions to refine the final design choices.

Furthermore, the approach differs depending on the type of propulsion that is accounted for: while in the case of impulsive propulsion the 'patched conics approach' can be used and the trajectory can be solved in closed form, in the case of low-continuous

thrust the trajectory cannot be obtained in closed form and it must be computed together with the thrust profile, resorting to optimization techniques.

There are different approaches to solve an optimal control problem (the direct method, the indirect method or the stochastic methods) and sometimes they can be combined to obtain a more accurate solution.

In general, the optimization procedure consists of defining the best control law, aiming at minimizing an objective (or cost) function, that could be the total speed increment  $\Delta V$  required for the mission in case of impulsive propulsion or the propellant consumption in case of low-thrust missions.

In the present paper, a general-purpose design code for interplanetary mission design is presented. The results are compared with the ones obtained from the optimal control software FALCON.m developed at the Institute of Flight System Dynamics of Munich [1]. In the current version of the tool, the numerical solver used by the latter is IPOPT (Interior Point OPTimizer) [2].

## 2 Problem Formulation

As mentioned above, to design an optimal interplanetary mission means to find the best control law able to minimize an objective function and this objective function is strictly related to the type of propulsion system.

In the case of impulsive propulsion, it is possible to use the square of the hyperbolic excess speed

needed to start the interplanetary travel, usually referred to as  $C_3$ , or directly the total speed increment  $\Delta V$ .

Considering a low-thrust propulsion system, an additional choice needs to be made: is the specific impulse kept constant (CSI system) or is allowed to vary during the space travel to reduce the propellant consumption (VSI system)? The performance index can be expressed as:

$$J = \int_{t_0}^{t_1} a dt \quad (\text{for CSI}) \quad (1)$$

$$J = \frac{1}{2} \int_{t_0}^{t_1} a^2 dt \quad (\text{for VSI}) \quad (2)$$

where  $a$  is the acceleration (i.e., the ratio between the thrust  $T$  and the spacecraft mass  $m$ ) profile.

It is possible to demonstrate that minimizing the cost function  $J$  means to minimize the propellant consumption. In fact  $J$  is strictly related to the parameter  $\gamma$  by the following formula:

$$\gamma = \sqrt{J\alpha} = m_p/m_i \quad (3)$$

where  $\alpha$  is the specific mass of the generator.

In the case of VSI, it is possible to show that minimizing  $\gamma$  leads also to a minimum value of the sum of the propellant and the generator mass, i.e. to a maximization of the payload. Consequently, for a low-thrust system the performance index can be written as:

$$J = \frac{m_p}{m_i} \quad (4)$$

Further details are given in [3-8].

Once the propulsion system has been chosen and  $J$  has been stated, a graphical overview of the various alternatives can be obtained. The cost is computed as a function of the starting and arrival dates so that a reasonable trade-off can be reached. A contour plot of the surface  $J(T_s, T_a)$  can thus be plotted.

As an alternative, instead of the arrival time  $T_a$ , it is possible to refer to the travel time  $T$ .

A grid is stated in the  $(T_s, T_a)$  plane – or in the  $(T_s, T)$  plane –, and the cost is computed at each point of the grid. The contour plot of the surface so obtained is represented and the relevant design decisions can be taken.

In the case of impulsive propulsion this contour plot is commonly called “pork-chop” plot [9] and an example is shown in Fig. 1: the cost function is  $C_3$  and the interplanetary travel is from Earth to Mars. The  $T_s$  interval is from August 2035 to December 2038 (i.e. from 400 days before to 1200 days after the 2035 opposition) with an interval of 2 days (800 values of  $T_s$  are thus considered). The  $T$  interval is between 40 and 600 days (280 values). As a consequence, the total number of missions that have been computed is 224.000 and the computer time on a Windows PC using a purposely written Matlab code is about 45 hours. The surface has 4 minima in the zone plotted, and the contour lines value of  $C_3$  span from 12 to 1500  $\text{km}^2/\text{s}^2$ ; higher values are not reported.

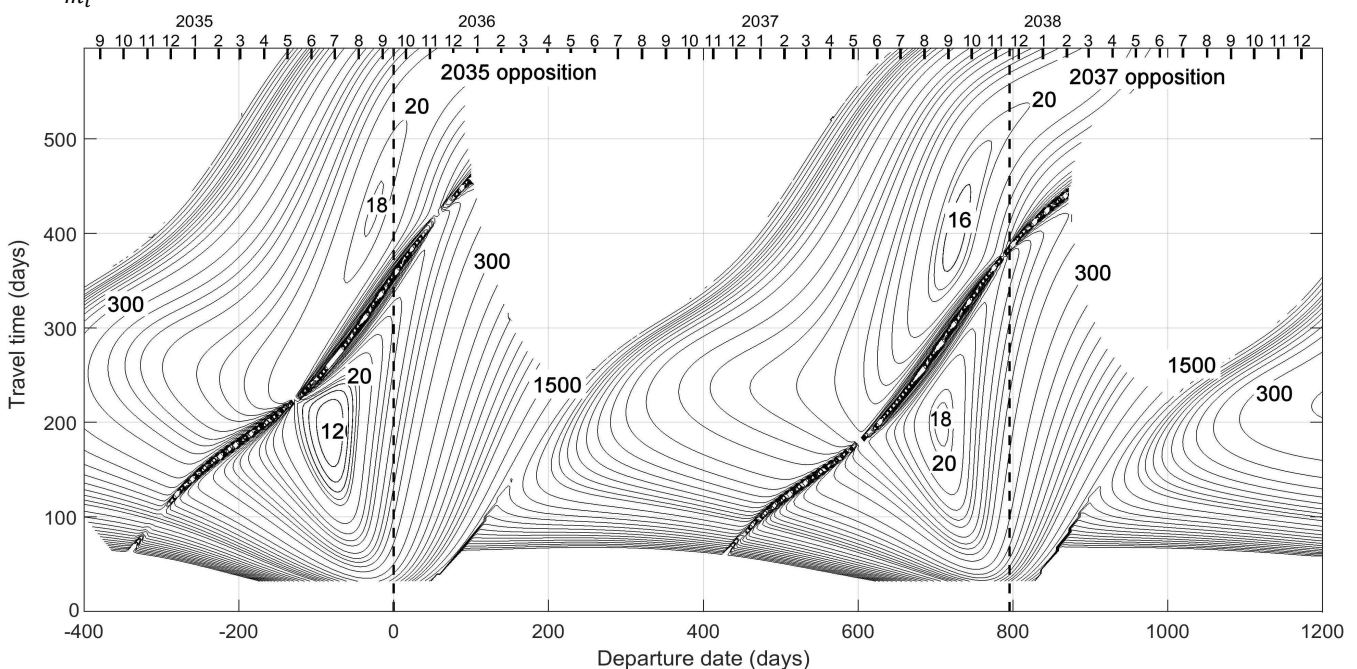


Fig. 1. Contour plot of the surface  $C_3(T_s, T)$  for an Earth-Mars mission in the 2035 and 2037 launch opportunities.  $C_3$  is expressed in  $\text{km}^2/\text{s}^2$ .

The plot has been obtained computing the planetary orbits following the JPL ephemerides [10].

Identifying the zones around the minima is an important result. For instance, if a launch in the 2035 opportunity (one of the most favourable) has to be performed, it is clear that the travel time allowing to perform the mission in the optimal conditions is about 200 days, but it is possible to reduce the travel time to about 160 days with a very small increase of cost: quite an important achievement. The following launch opportunity is much worse, both in terms of the possibility of reducing the travel time and in terms of cost.

The contour plot  $C_3(T_s, T_a)$ , quite similar to that of the figure, is usually referred to as a ‘pork-chop plot’.

The plot in the figure considers only the hyperbolic excess speed to start the interplanetary trajectory, and thus it is unique: no other plot for that span of  $T_s$  exist. However, it doesn’t tell the whole story, since the actual  $\Delta V$  required for performing the mission is not considered. To consider the whole mission is possible, but several design choices must be stated in advance:

- whether a direct launch is performed or, more likely, a parking orbit is used,
- what are the relevant orbit parameter,
- whether at the arrival an aerocapture or aerobraking manoeuvre is performed or, if an

orbit insertion at arrival is stated,

- what are the orbit parameters, etc.

A total mission  $\Delta V$ -plot can thus be obtained, but such a plot is not general and can be computed only after the mission has been already partially stated.

The case of low thrust missions is more complicated, since the process to obtain the trajectory and the thrust profile is much more computationally intensive. A contour plot of the surface  $J(T_s, T)$  can nevertheless be obtained in a fairly straightforward way, through any of the indirect or direct methods currently used.

A point which complicates the study in this case is that, when the whole mission is considered (orbit-to-orbit computation, since low thrust devices cannot start from the planetary surface), the interplanetary phase of the travel is preceded by a spiral phase about the starting planet – and followed by one around the arrival planet if no aerodynamic manoeuvre is done. Since these phases have a duration which can be comparable with that of the interplanetary phase, the relative duration of the three phases must be optimized. The computation must thus start by computing the surface  $J(T_s, T)$  for the interplanetary cruise. The planetocentric phases must then be computed. And the two (or three) phases must be combined so that the orbit to orbit  $J(T_s, T)$  contour plot is obtained.

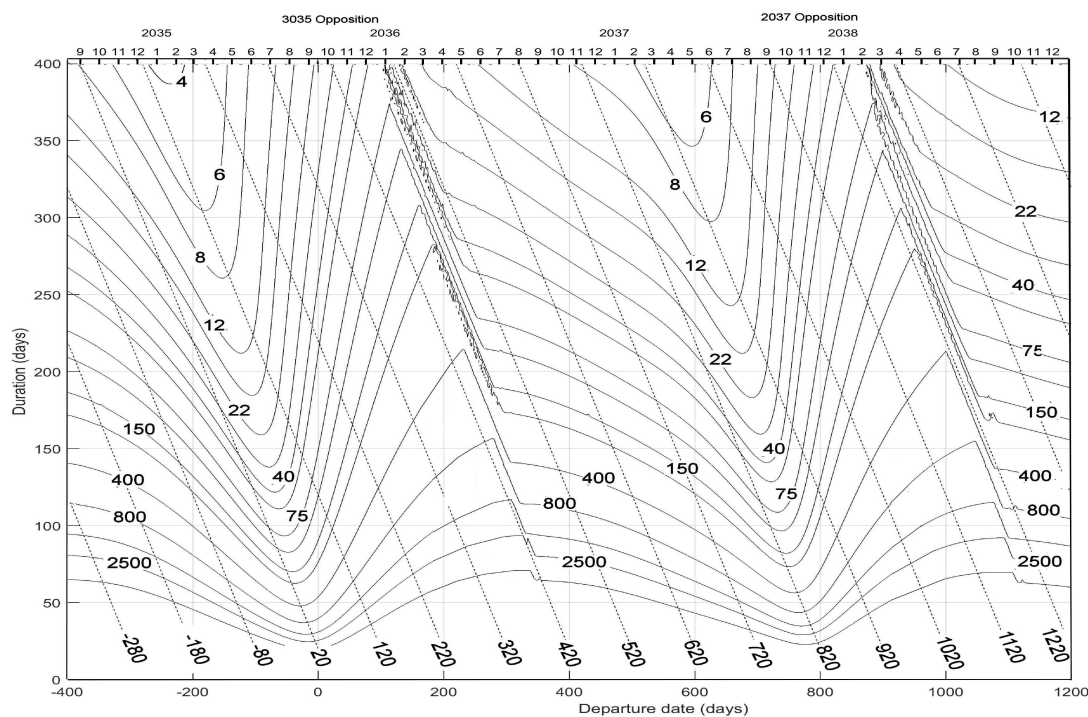


**Fig. 2. Earth-Mars J-plot for the same starting date interval as that of Fig. 1 – NEP with an ideal thruster with no limitation to the specific impulse. The values of  $J$  are expressed in  $m^2/s^3$ .**

An example of this orbit-to-orbit J-plot is shown in Fig. 2. It deals with the same time intervals shown in Fig. 1 but this time the starting and arrival orbits have been stated.

The plot has been computed assuming Nuclear Electric Propulsion (NEP) and an ideal thruster with no limitations on the specific impulse. The starting circular Earth orbit has an altitude of 800 km, and the arrival orbit about Mars is much elliptical, with a periareion at 320 km and an apoareion at 35,000 km.

The spiral phases to leave the starting planet and to approach the arrival ones should be optimized using specific codes. In the following, for these parts of the space travel, the assumption introduced by Edelbaum and based on the smallness of the angle between the tangent to the trajectory and the normal to the line connecting the spacecraft and the centre of the planet is used [6, 11-12].

The first difference between the two figures is that in Fig. 2 no closed contour lines exist, showing that the surface has no minima. The energy required for the mission decreases monotonically with increasing mission time, showing that it is possible to build very efficient slow cargo ships. Once a plot of the type reported above is obtained, a first choice

can be made regarding the starting and arrival dates and the energy requirements of the mission. At this point it is possible to proceed to refine the study, by introducing the perturbations due to the other planets of the Solar systems (n-body problem) and, if needed, also the perturbation due to the pressure of the light from the Sun.

### 3 Implementation

#### 3.1 General code structure

The formulation described in section 2 was used to implement a code, based on the MatLab environment, called IRMA (InteRplanetary Mission Analysis). To make the code more user friendly, it is provided of a number of Graphic User Interfaces (GUIs). The initial GUI is shown in Fig. 3. The upper left part allows the user to define the starting and the arrival planet and also, in the case of impulsive propulsion, a possible planet supplying gravity assist. The user can also chose whether the planetary orbits are assumed to be circular or elliptical, and in the latter case he must state the launch opportunity by supplying the year of the relevant planetary opposition.

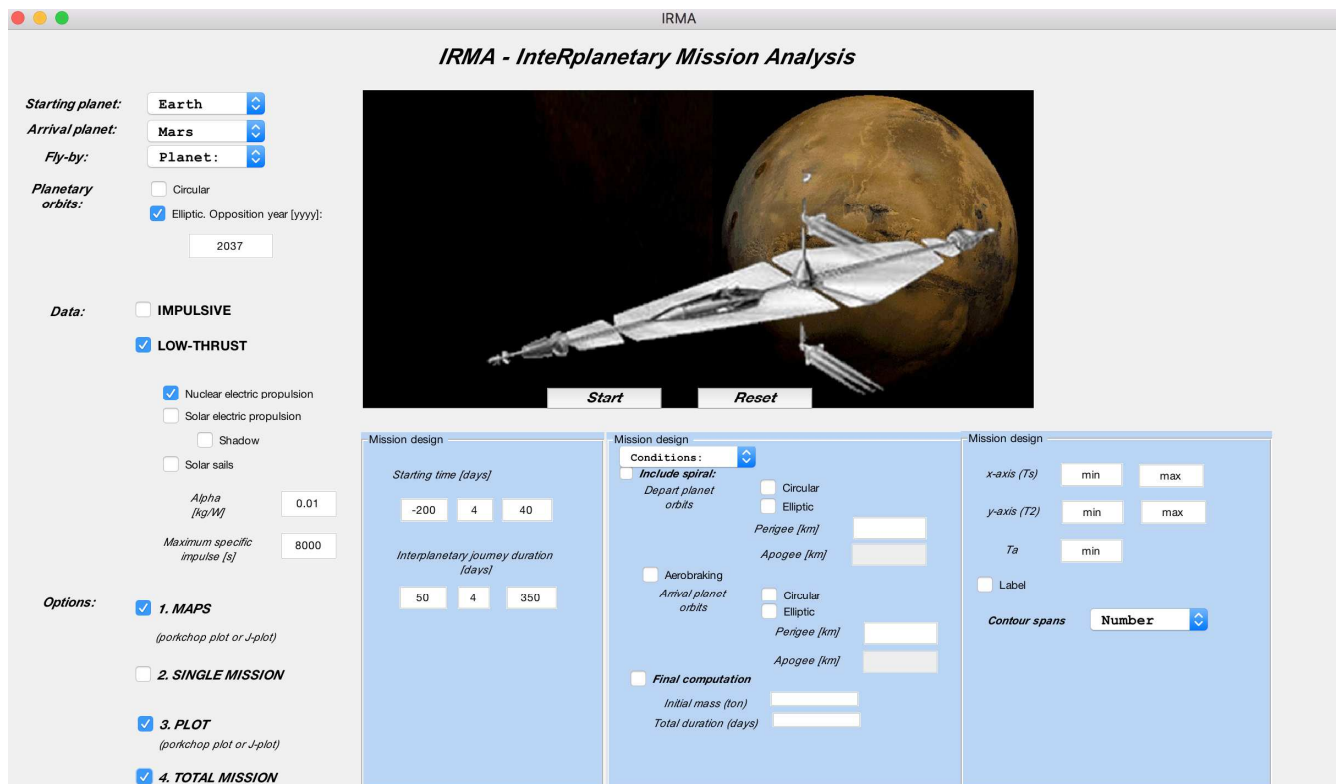


Fig. 3. Initial GUI of the MatLab IRMA code.

The central part allows the user to choose whether the spacecraft is propelled by an impulsive

of low thrust system and, in the second case, to choose between NEP, SEP – and in this case it is

possible to state whether to account for the interruption of the thrust when the spacecraft is in the shadow of the planet during planetocentric phases – or solar sail.

In addition, the user can decide to account for the limitations of the specific impulse due to the thrusters, and in this case also the specific mass of the generator must be stated.

Finally, the lower part allows to choose between 4 options:

- Computing and plotting the maps. In this case a further GUI (shown in the figure immediately at the right of the previous one) is opened, allowing to choose the  $T_s$  and  $T$  intervals. In case of low thrust propulsion here only the interplanetary part of the mission is accounted for.
- Studying a single mission. A new window is opened, to supply all the required data (not shown in the figure), like the exact starting date, the travel time, etc. Also here, only the interplanetary part of the mission is computed for low thrust propulsion. A GUI to supply the relevant starting and arrival data is shown at the right of the previous one.
- Plotting the diagrams previously computed, tailoring the scales and the other graphical choices to suit the user's choices (the relevant GUI is at the extreme right of the figure).
- Computing the J-plot or studying a single mission, but taking into account also the planetocentric phases. The same window allows to compute the mission taking into account the general n-body problem.

### 3.2 Some mathematical details

The positions of the planets are obtained from the JPL ephemerides as described in [10]. The ephemerides are pre-computed, and then are loaded by the relevant routines when required.

For the case of low thrust, the problem to be solved is finding the elliptical orbit, passing through points  $\mathbf{r}_1$  and  $\mathbf{r}_2$  (obtained from the ephemerides) in two instants separated by time  $T$ . It is a well known mathematical problem, known as the Gauss problem. It involves the solution of a nonlinear set of equations and here the approach based on the Newton-Raphson technique for solving nonlinear equations described by Shefer [13] is used.

If the trajectory includes a gravity assist manoeuvre, the interplanetary journey is subdivided into two parts, and a number of solutions obtained with different flyby times are computed. Then for each one of them the hyperbolic excess speed when starting and ending the flyby are computed, and the

solution in which the two velocities are equal is chosen. This doesn't allow to compute motorized flybys, but this is considered a small drawback.

In case of low continuous thrust, the indirect method described in [11] is used. The specific impulse is assumed as variable, at first with no limitations. The state space formulation of the problem, based on 12 first order ODEs is:

$$\left\{ \begin{aligned} \dot{v}_x &= -\frac{\mu x}{\sqrt{(x^2 + y^2 + z^2)^3}} + q_x \frac{r_E}{\sqrt{x^2 + y^2 + z^2}} \\ \dot{v}_y &= -\frac{\mu y}{\sqrt{(x^2 + y^2 + z^2)^3}} + q_y \frac{r_E}{\sqrt{x^2 + y^2 + z^2}} \\ \dot{v}_z &= -\frac{\mu z}{\sqrt{(x^2 + y^2 + z^2)^3}} + q_z \frac{r_E}{\sqrt{x^2 + y^2 + z^2}} \\ \dot{v}_{qx} &= -\mu \frac{q_x(-2x^2 + y^2 + z^2) - 3q_yxy - 3q_zxz}{\sqrt{(x^2 + y^2 + z^2)^5}} \\ \dot{v}_{qy} &= -\mu \frac{-3q_xxy + q_y(x^2 - 2y^2 + z^2) - 3q_zyz}{\sqrt{(x^2 + y^2 + z^2)^5}} \\ \dot{v}_{qz} &= -\mu \frac{-3q_xxz - 3q_yyz + q_z(x^2 + y^2 - 2z^2)}{\sqrt{(x^2 + y^2 + z^2)^5}} \\ \dot{x} &= v_x \\ \dot{y} &= v_y \\ \dot{z} &= v_z \\ \dot{q}_x &= v_{qx} \\ \dot{q}_y &= v_{qy} \\ \dot{q}_z &= v_{qz} \end{aligned} \right. \quad (5)$$

where in case of NEP  $\mathbf{q}$  is the ratio between the thrust and the mass of the spacecraft, while in case of SEP

$$\mathbf{q} = \frac{\mathbf{T}}{m} \sqrt{\frac{1}{f(|\mathbf{r}|/R_E)}} \quad (6)$$

and  $f(|\mathbf{r}|/R_E)$  is a function expressing the decrease of the power supplied by the solar arrays with increasing distance from the Sun.

In the simplest case the power decreases with the square of the distance, but more elaborate laws aimed at accounting for the increase of the efficiency of the solar arrays with the increase of the distance from the Sun – due to the decrease of the

temperature – can be found in the literature [14-16].

Once the boundary conditions on position and velocity are stated, an initial approximated solution is computed to start the iteration procedure solved by the BVP5C Matlab routine, based on the four-stage Lobatto IIIa formula and implemented as an implicit Runge-Kutta formula [17].

The objective function to minimize is given by

$$J = \frac{1}{2} \int_{t_0}^{t_1} q^2 dt . \quad (7)$$

If an upper limit on the specific impulse is set, the following assumption is made: the available power increases and it is maintained at his maximum value until the specific impulse exceeds the upper limit. At this point the specific impulse remains constant and the power decreases to maintain the thrust at the same value as it would have been obtained if no limitations were present.

This implies that no coast arcs are introduced (the thruster is never switched off) but at the same time the operations are made not at the optimal power level. Operating in this way a non-optimal solution is obtained, but one which is often quite close to the optimal one.

To show how much the present solver allows to obtain results close to the optimal one in the various cases, in the following examples the results obtained using the IRMA solver are compared with the optimal results obtained by the FALCON.m code.

In particular, FALCON.m uses direct discretization methods combined with gradient based numerical optimization and automatic analytic differentiation to solve the problem. The numerical optimization algorithm is provided by IPOPT. The formulation of the problem is different in case of unlimited and limited specific impulse.

In both cases the chosen performance index to minimize is  $J = \frac{m_p}{m_i}$ , but in the first case the problem consists of finding the optimal control law for the control vector  $u = [q_x, q_y, q_z]$  (the same performed by IRMA) while in the latter case the control vector is given by  $u = [P, I_{sp}]$ .

Further mathematical details are given in [18-19].

It is important to remark that if the simplified assumption made by IRMA is introduced, the term  $J$  loses the meaning of performance index. In fact, once the thrust law that is optimal for the unlimited operations has been obtained, the goal of the computation is to find a new value of the power and

a new value of the parameter  $J$  that is proportional to the propellant consumption able to maintain the desired thrust profile.

## 4 Examples

### 4.2 Long-stay mission to Mars

Consider a long-stay mission to Mars performed in the 2037-2040 launch opportunities with chemical propulsion. It is a minimal mission, with aero-braking both at the arrival to Mars and at the return to Earth, similar to that described in the NASA reference architecture 5.0 [20].

The pork-chop plots and the dates for the forward and backward journeys, looking for a compromise between minimum energy and short travel time, are first obtained. The ‘best’ choices are reported in Tab. 1.

**Tab. 1. Long-stay Mars mission. Starting times of the outbound and inbound travel (in days, referred to the opposition), and corresponding values of  $C_3$  (in  $\text{km}^2/\text{s}^2$ ), and  $\Delta V$  (in  $\text{m/s}$ ).**

	$T_s$	$T$	$C_3$	$\Delta V$
Outbound	-84	175	17.97	3,976.5
Inbound	-148	193	16.54	1,713.6

The starting orbit is a LEO at 400 km altitude, while the orbit around Mars is a highly elliptical orbit with a periareion an 320 km and an apoareion at 34,000 km.

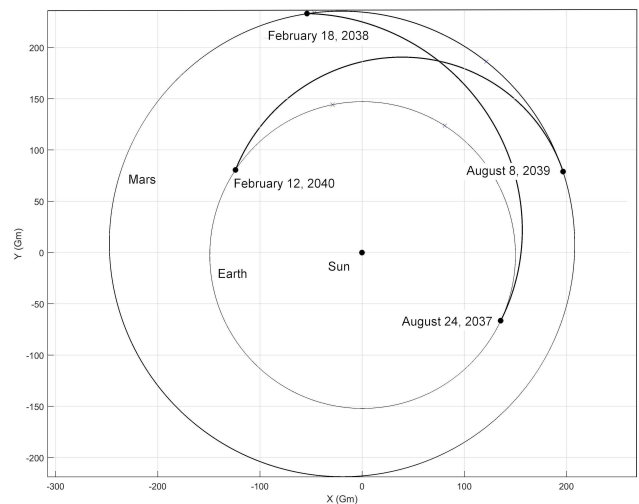


**Fig. 4. Trajectories for the outbound and the inbound legs of the mission.**

The trajectories are reported in Fig. 4. Assuming it is a split mission (the cargo and the return vehicle are sent separately from the crew), the mass budget of the crew ship and the return ship are reported in

Tab. 2. The values were computed using the  $\Delta V$  reported in Tab. 1, assuming cryogenic propellants.

**Tab. 2. Mass budget of the crew ship and the return ship (in t).**

	Dry+payload	Propellant	Total
Outbound	16	24.2	40.2
Inbound	18	8.8	26.8

From Tab. 1 it is clear that the 2037 launch opportunity is not a very favourable one (much worse than the 2035 launch opportunity, but better than the 2040 one). The results obtained are similar but not identical to those reported in [20], owing to some different design choices.

### 4.2 NEP Long-stay mission to Mars

Consider now a mission similar to the previous one, but performed using Nuclear Electric Propulsion. (NEP). The electric thrusters are assumed to be of the VASIMR type [21], fed with liquid argon. The maximum specific impulse is assumed to be 8000 s.

The overall efficiency of the thrusters plus the power conditioning is assumed to be 0.6, so that the effective value of the specific mass of the generator is  $\alpha = 10$  kg/kW (that of the generator alone is 6 kg/kW, a fairly optimistic value, but one that can be assumed for a not too far future).

The ship starts from an 800 km Earth orbit and at arrival it enters in an elliptical Mars orbit of the same type than that seen in the previous example. All manoeuvres are performed using the electric thrusters, and the only aerodynamic manoeuvres are the Entry, Descent and Landing (EDL).

First the J-plots for both the outbound and the inbound travels are plotted, and then the computation is repeated to take into account the spiral planetocentric parts of the trajectory. A trade-off between the value of  $J$  and the travel duration is performed, assuming a total travel time of 190 days for the outbound and 210 days for the inbound. The results are reported in Tab. 3.

**Tab. 3. Long-stay NEP Mars mission. Dates of the outbound and inbound travel (in days) referred to the 2037 opposition, and corresponding values of  $J$ , expressed in  $m^2/s^3$ . Also the ratio between the propellant mass and the initial mass is reported.**

	$T_s$	$T$	$J$	$m_p/m_i$
Outbound	-78	190	24.694	0.497
Inbound	-99	210	21.388	0.462

The trajectories are reported in Fig. 5, together with the dates of the various parts of the journey.

The computations were performed using IRMA.

If some limitations on the admissible values of the specific impulse are introduced, a bang-bang control law arises from the optimal control theory and a coasting part of the trajectory is so introduced. Nevertheless, in IRMA it is possible to approximate the optimal solution with a sub-optimal one assuming that the thrust is kept at the same values computed in the case of unlimited specific impulse, by increasing the maximum power available and by reducing it when the specific impulse exceeds the admissible values without ever switching off the thruster.

The results so obtained are reported in Tab. 4 and are compared with the optimal ones computed using the FALCON.m and the comparison is done on the interplanetary part of the trajectory, assuming  $I_{s\ max} = 8000$  s.

The time histories of the acceleration, the specific impulse, the thrust and the exhaust power are plotted in Fig.6 and Fig.7.

From Tab. 4, it is clear that, in the case of unlimited specific impulse, the solution found by IRMA is ‘more optimal’ than that found by FALCON.m by 2.7% in the outbound journey, while is ‘less optimal’ by 2.56% in the return journey. Clearly this must be attributed to the approximations with which both codes obtain the optimal solution.

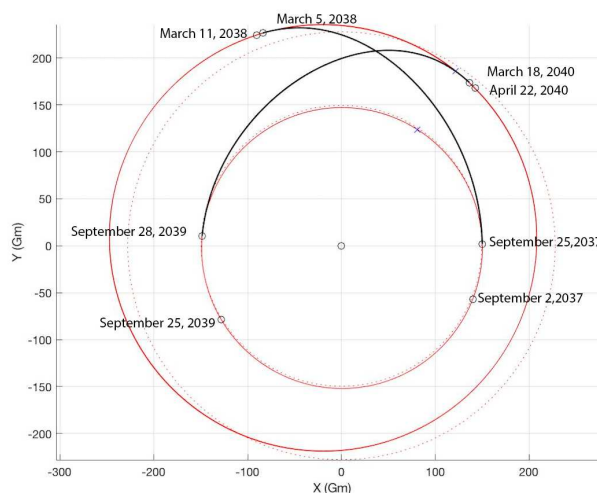


**Fig. 5. Trajectories for the outbound and the inbound legs of the mission.**

The strategy used by IRMA (reducing the power) cause an increase of propellant by 1.92% against the 0.97% obtained from strategy used by FALCON.m (switching of the thruster) in the outbound travel. The same values are 1.83% and 0.77% in the return journey. The difference is quite small, particularly if

it is considered that the limitation of the specific impulse affects almost half of the travel time.

**Tab. 4. Long stay NEP Mars mission. Comparison with FALCON.m results for unlimited specific impulse mission ( $m_p/m_i^*$ ) and limited specific impulse mission ( $m_p/m_i$ ).**

	Outbound		Inbound	
	$m_p/m_i^*$	$m_p/m_i$	$m_p/m_i^*$	$m_p/m_i$
IRMA	0.3483	0.3550	0.3439	0.3502
FALCON.m	0.3576	0.3611	0.3351	0.3377
$\epsilon$ (%)	-2.67	-1.72	2.56	3.57

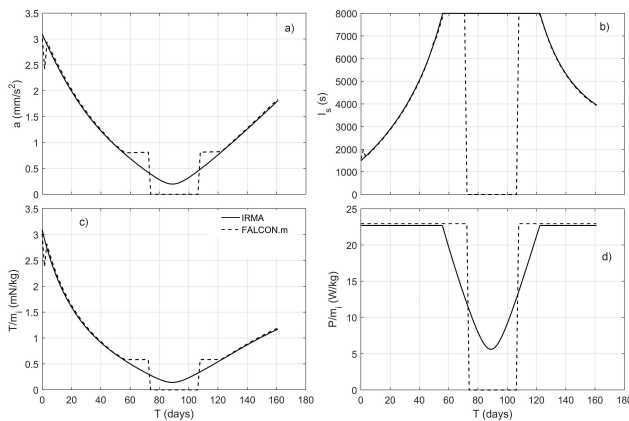


**Fig. 6. Comparison of the results obtained from IRMA and FALCON.m. Time histories of a): acceleration, b): specific impulse, c): thrust, d): exhaust power.**

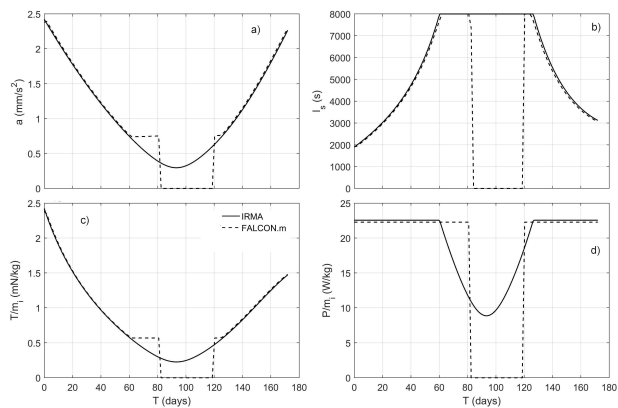


**Fig. 7. Same as Fig. 6 , but for the return journey**

It must be expressly noted that in both cases parameter  $J$  cannot be any more computed using Eq. (2), while retaining the meaning of a parameter proportional to the square of  $m_p/m_i$ .

**4.3 NEP very fast space ship to Mars**

Consider a fast spacecraft used to carry people to Mars. Assume that a very advanced technology is available, likely a fusion nuclear generator and a variable specific impulse thruster capable of a very

high value specific impulse (the former is not of great use without the second).

The specific mass of the generator is assumed to be  $\alpha=0.014 \text{ kg/kW} =14 \times 10^{-6} \text{ kg/W}$ , a value that at present belongs more to science fiction than to actual possibilities. This example is shown to state that very fast interplanetary journeys do not require questionable breakthrough like warp drives or propellantless propulsion, but simply a gradual development of present technologies. This value of  $\alpha$  requires new materials and technologies, but not unpredictable theoretical developments.

Also the electric thrusters are assumed to be more developed than present ones, having an improved efficiency  $\eta = 0.7$ , and a higher maximum specific impulse  $I_{s \text{ max}} = 15,000 \text{ s}$ . The overall specific mass is thus  $\alpha = 0.02 \text{ kg/kW}$ .

The passenger ship starts from an 800 km LEO, and arrive in an equally circular 300 km LMO.

The launch opportunity is assumed to be that of 2069 and the total travel time is 40 days. The optimal durations of the various phases of the Earth-Mars journey are:

- First phase:  $T_1 = 0.7 \text{ days}$ ,  $J_1 = 264.0 \text{ m}^2/\text{s}^3$
- Second phase:  $T_2 = 39 \text{ days}$ ,  $J_2 = 6713.2 \text{ m}^2/\text{s}^3$
- Third phase:  $T_3 = 0.3 \text{ days}$ ,  $J_3 = 92.9 \text{ m}^2/\text{s}^3$
- Total:  $T = 40 \text{ days}$ ,  $J = 7070.1 \text{ m}^2/\text{s}^3$ ,  $\gamma = 0.376$ .

The trajectory is reported in Fig. 8.

The values of  $J$  and of the propellant, generator and propellant+generator mass fractions are reported in Tab. 5, computed only with reference to the interplanetary part of the journey (owing to the very fast transfer, the planetocentric parts are almost negligible in comparison with the interplanetary part)

If there is no limitation to the specific impulse, the results obtained using the two solvers are almost coincident.

On the contrary, if the specific impulse is limited to 15,000 s the two strategies yield quite different results. The strategy used by the IRMA solver, reducing the power while maintaining always the thruster on, leads to a larger propellant consumption. The strategy used by the FALCON.m solver, is much more convenient for what the propellant consumption is concerned: the value of  $\gamma$  is almost halved.

As shown in Fig. 9, where the time history of the acceleration, the specific impulse, the thrust and the exhaust power are plotted, the strategy used in FALCON.m leads to quite short propulsive phases at the beginning and at the end of the interplanetary transfer, with a very long coast phase between them. In a way, it is possible to state that the bang-bang



opportunity and another one due to the very elliptical and inclined orbit of Pluto. In this example the launch opportunity of 2060 is considered.

The performance of the generator and the thruster are summarized as:

- $\alpha_{gen} = 3.5 \text{ kg/kW}$
- $\eta = 0.7$
- $I_{s \text{ max}} = 10,000 \text{ s}$
- $\alpha = 5 \text{ kg/kW}$ .

The durations of the 3 phases and the values of J are:

- First phase:  $T_1 = 77.5 \text{ days}$ ,  $J_1 = 3.593 \text{ m}^2/\text{s}^3$
- Second phase:  $T_2 = 2166.5 \text{ days}$ ,  $J_2 = 79.34 \text{ m}^2/\text{s}^3$
- Third phase:  $T_3 = 5.9 \text{ days}$ ,  $J_3 = 0.304 \text{ m}^2/\text{s}^3$
- Total:  $T = 2250 \text{ days}$ ,  $J = 83.237 \text{ m}^2/\text{s}^3$ ,  $\gamma = 0.645$

The journey is performed almost always in constant specific impulse conditions, since the optimal specific impulse is much higher than that

allowed by the thruster. If it were possible to travel in optimal specific impulse conditions,  $J_2$  would have been less than half:  $34.115 \text{ m}^2/\text{s}^3$ .

The results concerning the interplanetary travel are shown in Tab 6.

Assuming a dry plus payload mass of 10 t, the propellant mass would be 51.41 t, the generator mass of 18.22 t, for a total mass of 79.63 t.

The projection of the trajectory on the ecliptic plane is plotted in Fig. 10 (the trajectory actually departs much from the ecliptic plane, due to the inclination of Pluto orbit).

In case of unlimited specific impulse the results are very close to each other. In case of limited specific impulse, the strategy of reducing the power seems to be more convenient than that of switching it off altogether.

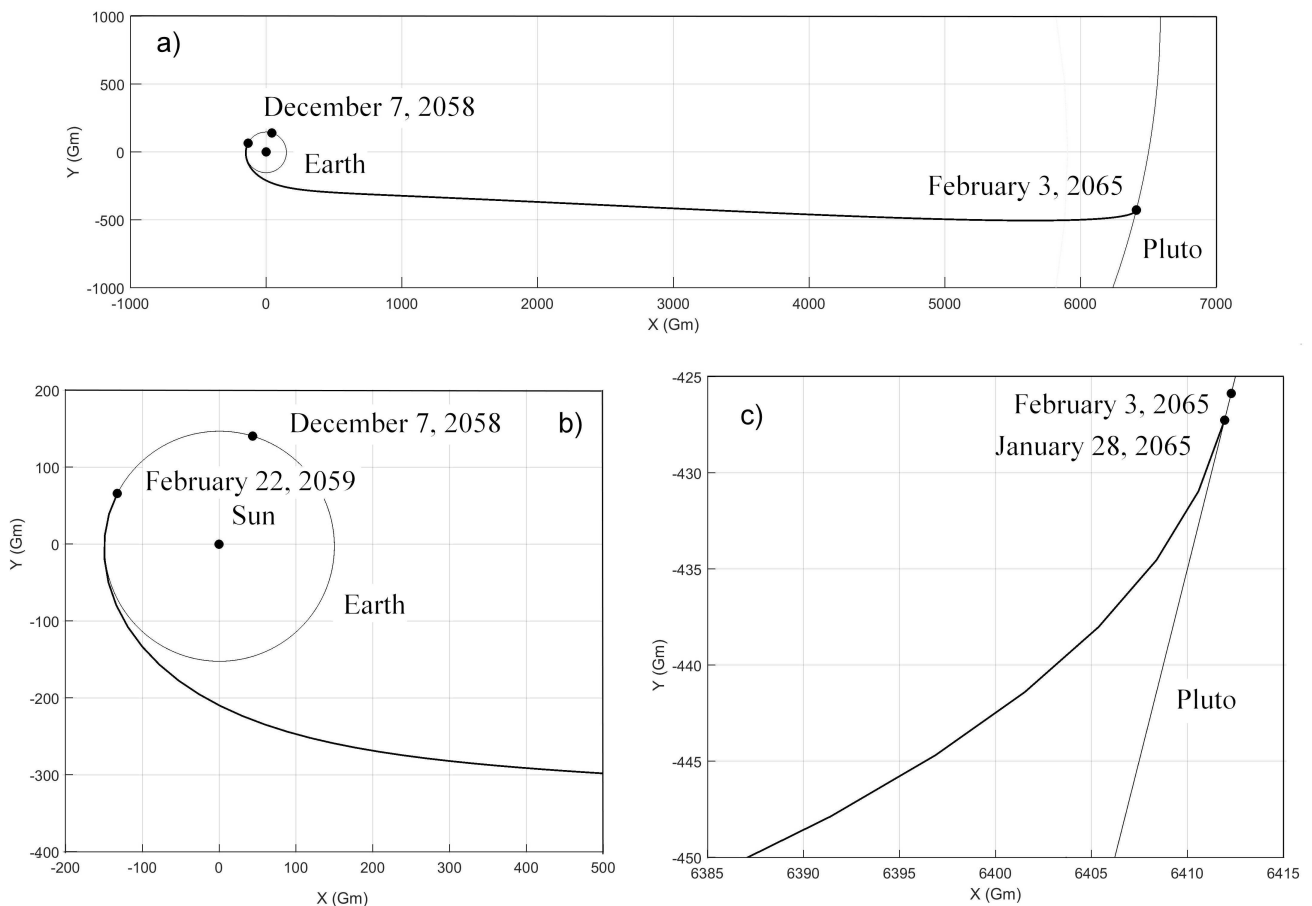


**Fig. 10. Trajectory for the Pluto NEP probe. A): overall trajectory, b): trajectory close to Earth, c) Trajectory close to Neptune (note the approximations in the graphic representation).**

This can be attributed to the fact that, as shown below, the FALCON.m solver finds a solution in which there are two coasting arcs, with a powered phase in between them. Further investigations should be performed to see whether this is actually a

global minimum (and the results obtained by IRMA suggest this is not the case) or just a local minimum.

The time history of the acceleration and of the specific impulse during the interplanetary phase are plotted in Fig.11.

With a reasonable value of  $\alpha$  it is thus possible to put a satellite in orbit around Pluto (and to land a

**Tab. 6. NEP probe to Pluto: comparison between the values of  $J$  and mass breakdown (referred to the interplanetary cruise only), computed using IRMA and FALCON.m.**

		$I_s$ unlimited	$I_{smax}=10,000$ s
IRMA	$J$ ( $m^2/s^3$ )	34.115	79.34
	$\gamma = m_p/m_i$	0.413	0.6298
	$m_w/m_i$	0.2424	0.1697
	$(m_p+m_w)/m_i$	0.6554	0.7995
FALCON.m	$J$ ( $m^2/s^3$ )	33.5229	104.083
	$\gamma = m_p/m_i$	0.4094	0.7214
	$m_w/m_i$	0.2418	0.1692
	$(m_p+m_w)/m_i$	0.6512	0.8907

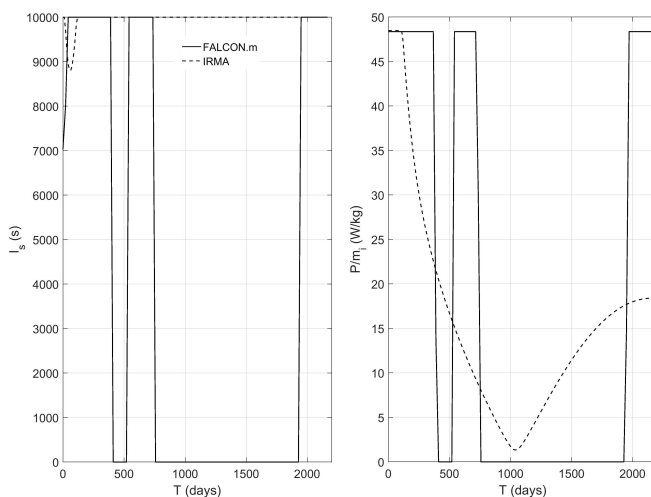


**Fig. 11. Comparison of the results obtained from IRMA and FALCON.m. Time histories of a): acceleration and b): Specific impulse.**

The optimal mass breakdown, taking into account the whole journey, planetocentric parts included, is the following:

	IRMA	FALCON.m
Payload+structure mass	10 t	10 t
Initial mass	53.97 t	105.49 t
Propellant mass	34.81 t	77.64 t
Power generator mass	9.16 t	17.85 t
Power of the generator	2.61 MW	5.10 MW

**5 Future developments of the code**

The IRMA code is a part of a self-funded, long term project at the Mechanical and Aerospace Engineering Dept. of Politecnico di Torino.

The following additions are being implemented (some of them are already running in a preliminary form):

rover on the planet) in just slightly more than 6 years, with a single launch of a heavy-lift rocket.

- Including propellantless propulsion. The cost parameter will be a parameter related to the mass of the propulsion system. For solar sails the sail area can be used, while for other, hypothetical, devices which use power to produce the thrust, it will include also the mass of the power generator.
- Implementing an utility to optimize two-ways travels, performed within a single launch opportunity, like short stay missions to Mars. This utility has already been implemented as a stand-alone code [22], and it will be soon integrated into IRMA.
- Going beyond the 2-body problem. This will be active only in the Single Mission or the Total Mission mode, since it would increase too much the computer time to perform the computation of a contour diagram.
- Including the perturbation to the trajectory due to the light pressure of the Sun. Since it is a small perturbation, it makes sense only if accounted for together with the presence of the gravitational attraction of many planets, and thus it will be available only in the same modes of the previous point.
- Implementation of the possibility of using a bang-bang strategy in all the computations performed by the code, and not only when computing single missions. This will be done by allowing to use the FALCON.m solver in any stage of the computation.
- Implementing an utility for computing directly the time included between two dates, to convert dates from Gregorian to Julian calendar or to a Martian calendar (or viceversa).

Other developments will be included if the users of the code will suggest further aspects of the design of interplanetary missions worth being included.

**5 Conclusion**

The present paper describes the IRMA (Interplanetary Mission Analysis) code developed by the authors. Its first aim is obtaining the contour plot of a suitable cost function (which depends on the propulsion type) as a function of the starting date and the travel duration. This plot allows to chose the starting and arrival time representing the best compromise between the journey duration and its cost.

Once the interplanetary part of the travel has been studied, the planetocentric departure and

arrival phases can be included in the computation, so that an orbit-to-orbit analysis can be performed.

Finally, a detailed analysis of the chosen journey can be obtained and later refined abandoning the two-body approximation and including further effects like the Sun light pressure.

The code has an internal solver, based on the Newton-Raphson method for impulsive thrust and on an indirect method for low thrust, but can resort also to external solvers, like the FALCON.m code based on a direct method. A comparison between different approaches and methods, can thus be made, to evaluate the reliability and accuracy of the various approaches in different applications.

#### References:

- [1] M. Rieck, M. Bittner, B. Grüter, and J. Diepolder. *FALCON.m User Guide. Institute of Flight System Dynamics*, Technical University of Munich, 2016. url: [www.falcon-m.com](http://www.falcon-m.com).
- [2] A. Wächter and L. T. Biegler. *On the Implementation of a Primal-Dual Interior Point Filter Line Search Algorithm for Large-Scale Nonlinear Programming*. In: *Mathematical Programming* Vol. 106. No. 1 (2006)
- [3] S. Kembler, *Interplanetary mission analysis and design*, Springer Science & Business Media, 2006.
- [4] J. Z. Ben-Asher. *Optimal Control Theory with Aerospace Applications*, AIAA Education Series. Reston, VA, USA: American Institute of Aeronautics and Astronautics, 2010. isbn: 978-1600867323.
- [5] J. T. Betts. *Practical Methods for Optimal Control and Estimation Using Nonlinear Programming. Second edition*, Advances in Design and Control. Philadelphia: SIAM, Society for Industrial and Applied Mathematics, 2009.
- [6] P. Marec, *Optimal Space Trajectories*, Elsevier, New York, 1979
- [7] Langmuir, D. B. (1959). *Low-thrust flight: Constant exhaust velocity*, in field-free space. Space technology.
- [8] Irving, J. H. (1959). *Low thrust flight: variable exhaust velocity*, in gravitational fields. Space Technology, 10.
- [9] G. R. Hintz, *Orbital mechanics and astrodynamics: techniques and tools for space missions*,. Springer, 2015.
- [10] E. M. Standish, *The JPL planetary and lunar ephemerides*, DE402/LE402. In *Bulletin of the American Astronomical Society* (Vol. 27, p. 1203), 1995.
- [11] P.W. Keaton, *Low Thrust Rocket Trajectories*, LA-10625-MS, Los Alamos, 2002.
- [12] G. Genta, P. F. Maffione, *Low Thrust Interplanetary Transfers: Second Approximation Computation of Planetocentric Phases*, *Advances in Aerospace Science and technology*, CSA,
- [13] A. Shefer, *New method of Orbit Determination from Two Position Vectors Based on Solving Gauss's Equations*, *Solar System Research*, Vol. 44, No. 3, pp. 252-266.
- [14] C. Circi, *Mars and Mercury missions using solar sails and solar electric propulsion*, *Journal of Guidance, Control, and Dynamics*, Vol. 27(3), 2004, pp. 496-498.
- [15] S. N. Williams and V. L. Coverstone-Carroll *Benefits of solar electric propulsion for the next generation of planetary exploration missions*, *The Journal of the Astronautical Sciences*, Vol. 45(2), 1997, pp. 143-160.
- [16] M. Kim, *Continuous Low-Thrust Trajectory Optimization: Techniques and Applications*, Virginia Polytechnic Institute and State University, Blacksburg, Virginia, 2005.1
- [17] Shampine, L.F., M.W. Reichelt, and J. Kierzenka, *Solving Boundary Value Problems for Ordinary Differential Equations in MATLAB with bvp4c*, [http://www.mathworks.com/bvp\\_tutorial](http://www.mathworks.com/bvp_tutorial).
- [18] Mengali, G., & Quarta, A. A. (2005). *Fuel-optimal, power-limited rendezvous with variable thruster efficiency*, *Journal of Guidance, Control, and Dynamics*, 28(6), 1194-1199.
- [19] Casalino, L., Colasurdo, G. *Optimization of variable-specific-impulse interplanetary trajectories*, *Journal of Guidance Control and Dynamics*, 27(4), 678-684, 2004.
- [20] B.G. Drake ed., *Mars Architecture Steering Group, Human Exploration of Mars, Design Reference Architecture 5.0* (and addendums), NASA Johnson Space Center, 2009.
- [21] Diaz, F. R. C.(2000). *The VASIMR rocket*, *Scientific American*, 283(5), 90-97.
- [22] G. Genta, P. F. Maffione, *Fast Human Mars Missions: what are the actual requirements*, 10th IAA Symposium on the Future of Space Exploration: Towards the Moon Village and Beyond, Torino, June 2017.
- [23] J. D. Anderson. *Fundamentals of Aerodynamics*, Fifth edition. McGraw-Hill Series in Aeronautical and Aerospace Engineering. New York: McGraw-Hill, 2011.
- [24] G. Genta, *Next Stop Mars: The Why, How and When of Human Missions*, Springer, New York, 2017.
- [25] G. Genta, P. F. Maffione, *Sub-optimal Low-thrust Trajectories for Human Mars Exploration*, *Atti dell'Accademia delle Scienze di Torino, Memorie Sc. Fis.*, 38-39 (2014-2015), pp 87-126.
- [26] G. Genta, P. F. Maffione, *Optimal Low-Thrust Trajectories for Nuclear and Solar Electric Propulsion*, *Acta Astronautica*, Vol. 118, p. 251-261, 2016.
- [27] G. Genta, P. F. Maffione, *Fast low thrust trajectories for the exploration of the outer solar system*, 9th IAA Symposium on The Future of

Space Exploration: Towards New Global Programmes, Torino, July, 2015.

[28] G. Genta, P. F. Maffione, *Quick interplanetary trajectories in presence of a space elevator*, 9th IAA Symposium on The Future of Space Exploration: Towards New Global Programmes, Torino, July, 2015.

[29] G. Mengali, A. Quarta. (2008). *Optimal trade studies of interplanetary electric propulsion missions*, Acta Astronautica, 62(12), 657-667.

*Symbols and achronyms:*

$m$  mass of the spacecraft  
 $\mathbf{r}$  distance of the spacecraft from the Sun  
 $C_3$  square of the hyperbolic excess speed  
 $J$  objective function

$R_E$  nominal radius of Earth orbit (1AU)  
 $S$  sail area  
 $T$  travel time  
 $\mathbf{T}$  thrust  
 $T_a$  arrival time  
 $T_s$  starting time  
 $\mu$  gravitational parameter of the Sun  
 $\Delta V$  speed increment  
 CSI Constant Specific Impulse  
 LEO Low Earth Orbit  
 LMO Low Mars Orbit  
 NEP Nuclear Electric Propulsion  
 SEP Solar Electric Propulsion  
 VSI Variable Specific Impulse